ELSEVIER

Journal of Organometallic Chemistry 551 (1998) 55–65

Journal of Organometallic Chemistry

Binuclear pentamethylcyclopentadienyl rhodium(III) compounds with pyrazolate and thiolate bridging ligands [1]

Juventino J. García [a,*], Gerardo Barón [a], Alma Arévalo [a], Hugo Torrens [a], Daniel Carmona [b,2], Montserrat Esteban [b], Fernando J. Lahoz [b], José A. López [b], Luis A. Oro [b,2]

[a] *Departamento de Química Inorgánica, Facultad de Química, Universidad Nacional Autónoma de México, 04510 México, D.F., Mexico*
[b] *Departamento de Química Inorgánica, Instituto de Ciencia de Materiales de Aragón, Universidad de Zaragoza–Consejo Superior de Investigaciones Científicas, 50009 Zaragoza, Spain*

Received 1 May 1997

Abstract

Binuclear thiolato-bridged complexes of general formula $[(\eta^5\text{-}C_5Me_5)_2Rh_2(\mu\text{-Pz})(\mu\text{-SR})_2]BF_4$ (Pz = pyrazolate; R = C_6F_5 (**2a**), $p\text{-}C_6F_4H$ (**2b**), $p\text{-}C_6H_4F$ (**2c**) or C_6H_5 (**2d**)) have been prepared by reacting the hydroxo–pyrazolato-bridged compound $[(\eta^5\text{-}C_5Me_5)_2Rh_2(\mu\text{-Pz})_2(\mu\text{-OH})]$ BF_4 with the corresponding thiol. Complexes **2a–d** show two types of fluxionality: rotation around the thiol C–S bond and isomerization among the three possible isomers in which the thiols occupy axial and/or equatorial positions within the Rh_2S_2 metallacycle. These processes are studied by ^1H and ^{19}F NMR spectroscopies. The crystal structures of **2b** and **2d** were established by X-ray crystallography. Compound **2b** crystallises in the monoclinic space group $P2_1/n$, with lattice parameters $a = 14.368(2)$, $b = 18.252(2)$, $c = 15.268(2)$ Å, $\beta = 109.79(1)°$ and $Z = 4$. Complex **2d** crystallises in a monoclinic lattice, space group $C2/c$, with $a = 48.723(5)$, $b = 8.7503(8)$, $c = 40.334(4)$ Å, $\beta = 112.620(5)°$ and $Z = 16$. Both cationic dinuclear complexes exhibit very similar molecular structures with analogous *pseudo*-octahedral environments for the rhodium centres. Each metal is bonded to a terminal $\eta^5\text{-}C_5Me_5$ group and to three bridging ligands: two monodentate thiolates ($p\text{-}SC_6F_4H$ in **2b** and SC_6H_5 in **2d**) and a bidentate pyrazolate group. The main structural dissimilarity affects the relative configuration of the thiolate phenyl substituents giving rise to *syn* (**2b**) or *anti* (**2d**) structures. © 1998 Elsevier Science S.A.

Keywords: Rhodium; Binuclear complexes; Pentamethylcyclopentadienyl; Pyrazolato; Thiolato

---

1. Introduction

The discovery of $[(\eta^5\text{-}C_5Me_5)MCl_2]_2$ (M = Rh, Ir) by Maitlis [1,2] has provided a relevant milestone on the development of organometallic chemistry and homogeneous catalysis for nearly three decades, resulting in major advances in the understanding of these areas. The η^5-pentamethylcyclopentadienyl group is an excellent protecting ligand towards rhodium and iridium, whilst replacement of the chlorine ligands occurs very easily, with a marked tendency to form binuclear complexes.

On the other hand, several laboratories have studied the ability of binucleating groups such as pyrazolate or thiolate ligands for the preparation of binuclear rhodium and iridium complexes containing the $M_2(\mu\text{-Pz})_2$ [3–5], $M_2(\mu\text{-SR})_2$ [6] or $M_2(\mu\text{-Pz})(\mu\text{-SR})$ [7] frameworks. Furthermore, our laboratories have independently reported the synthesis and reactivity of several pentamethylcyclopentadienyl rhodium and iridium complexes containing pyrazolato [8–11] or perfluorothiolato [12,13] groups as bridging ligands.

In this paper we report the synthesis and characterization of a new family of cationic binuclear complexes of formula $[(\eta^5\text{-}C_5Me_5)_2Rh_2(\mu\text{-Pz})(\mu\text{-SR})_2]BF_4$ that shows an interesting fluxional behaviour in solution.

---

[*] Corresponding authors.

[1] Dedicated to a spectacular scientist and a good friend and colleague, Peter M. Maitlis, on occasion of his 65th birthday.

[2] Also corresponding author.

0022-328X/98/$19.00

2. Results and discussion

2.1. Synthesis of the compounds

The compounds $[(\eta^5\text{-}C_5Me_5)_2Rh_2(\mu\text{-}Pz)(\mu\text{-}SR)_2]BF_4$, (Pz = pyrazolate) were prepared from the di-μ-pyrazolato-μ-hydroxo complex $[(\eta^5\text{-}C_5Me_5)_2Rh_2(\mu\text{-}Pz)_2(\mu\text{-}OH)]BF_4$ (**1**) [14] and thiol according to Eq. (1):

$$\begin{aligned}&\left[(\eta^5\text{-}C_5Me_5)_2Rh_2(\mu\text{-}Pz)_2(\mu\text{-}OH)\right]BF_4 + 2HSR\\&\quad\to\left[(\eta^5\text{-}C_5Me_5)_2Rh_2(\mu\text{-}Pz)(\mu\text{-}SR)_2\right]BF_4\\&\qquad + HPz + H_2O,\\&R = C_6F_5(\mathbf{2a}),\ p\text{-}C_6F_4H(\mathbf{2b}),\\&p\text{-}C_6H_4F(\mathbf{2c})\text{ or }C_6H_5(\mathbf{2d})\end{aligned}\qquad(1)$$

Most probably the reaction proceeds through intermediates of the types $[(\eta^5\text{-}C_5Me_5)_2Rh_2(\mu\text{-}Pz)(\mu\text{-}SR)(\mu\text{-}OH)]^+$ and/or $[(\eta^5\text{-}C_5Me_5)_2Rh_2(\mu\text{-}Pz)_2(\mu\text{-}SR)]^+$ with only one bridging thiolate ligand. However we have not detected any of them and, when the reaction was carried out with only one equivalent of thiol, a mixture of the corresponding complex **2** and unreacted starting compound **1** was obtained. Consequently, we assume that the rate of formation of complexes **2** from the mono-thiolate-bridged intermediates is greater than that of formation of the aforementioned intermediates from the starting compound **1**. Small amounts of the previously described cation–anion complexes $[(\eta^5\text{-}C_5Me_5)_2Rh_2(\mu\text{-}SR)_3][(\eta^5\text{-}C_5Me_5)Rh(SR)_3]$ have also been observed [15,16].

The new complexes are yellow-to-red crystalline solids, stable at room temperature, soluble in dichloromethane, chloroform and acetone and insoluble or sparingly soluble in diethyl ether, hexane or toluene. They were characterised by elemental analysis (see Section 4), IR and ^1H, ^{19}F and ^{13}C spectroscopy and by the X-ray crystal structure determinations on compounds **2b** and **2d**. The IR spectra revealed the absence of the ν(OH) vibrations of the starting compound. The ^1H and ^{19}F spectra, at room temperature, were consistent with the proposed stoichiometries and indicated, in all cases, that the complexes are fluxional. We will analyse this behaviour in detail below.

2.2. Molecular structures of $[(\eta^5\text{-}C_5Me_5)_2Rh_2(\mu\text{-}Pz)(\mu\text{-}S\text{-}p\text{-}C_6F_4H)_2]BF_4$ (**2b**) and $[(\eta^5\text{-}C_5Me_5)_2Rh_2(\mu\text{-}Pz)(\mu\text{-}SC_6H_5)_2]BF_4$ (**2d**)

In order to obtain structural information helpful to understand the different NMR fluxional behaviour observed for the apparently analogous complexes **2b** and **2d** (see below) we carried out the X-ray solid state analysis of these two compounds. Both crystal structures showed the presence of dinuclear cations and disordered BF_4^- anions packed within normal Van der Waals distances. In the case of **2d** two crystallographically independent set of atoms were identified in the structural determination. Figs. 1 and 2 display molecular drawings for the cations of **2b** and **2d**, respectively. Table 1 collects a list of selected bond distances and angles for these complexes.

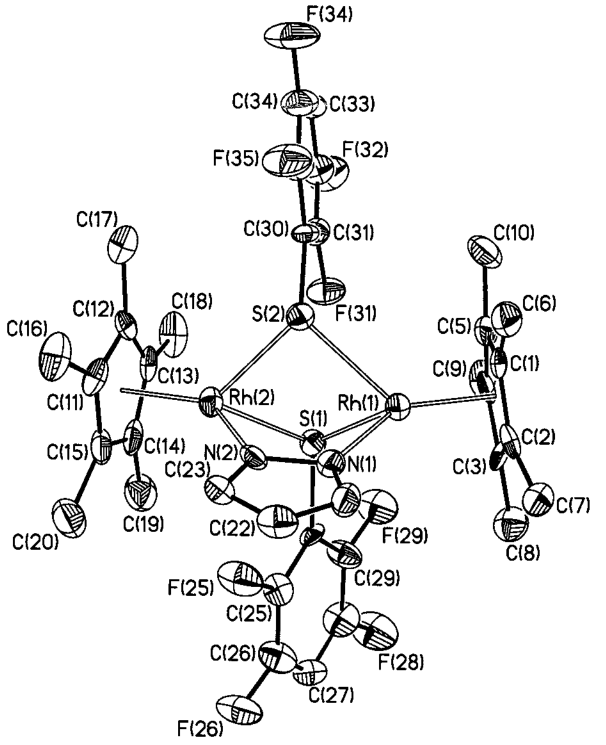

Fig. 1. Molecular representation of the cationic complex $[(\eta^5\text{-}C_5Me_5)_2Rh_2(\mu\text{-}Pz)(\mu\text{-}S\text{-}p\text{-}C_6F_4H)_2]^+$ with the labelling scheme used. Hydrogens have been omitted for clarity.

The molecular structures of the cations of **2b** and **2d** are rather similar. In both cases two $(\eta^5\text{-}C_5Me_5)$Rh moieties are maintained together through a triple bridge:

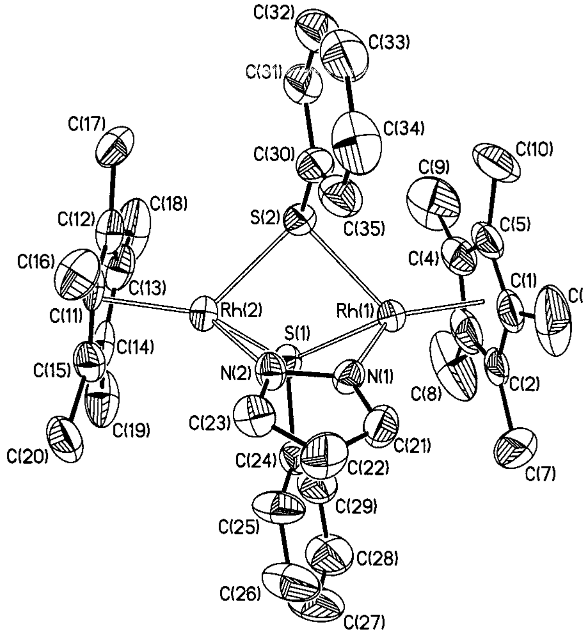

Fig. 2. Molecular drawing of the cation $[(\eta^5\text{-}C_5Me_5)_2Rh_2(\mu\text{-}Pz)(\mu\text{-}SC_6H_5)_2]^+$ of compound (**2d**) with the numbering scheme used.

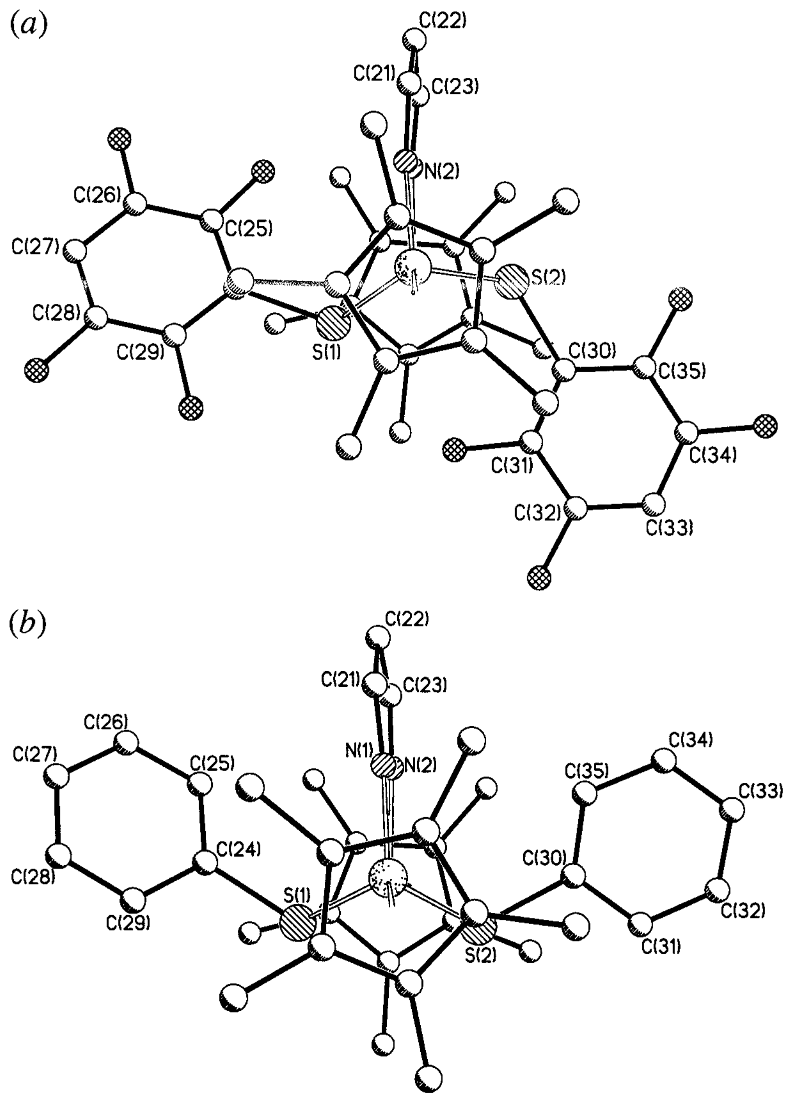

Fig. 3. Schematic representation along the Rh(1)–Rh(2) direction of the cationic complexes **2b** (*a*) and **2d** (*b*) showing the *anti* (**2b**) and *syn–exo* (**2d**) configuration of the thiolate phenyl groups.

a bidentate pyrazolate—coordinated as usual through its two nitrogen atoms—and a couple of *S*-bonded bridging thiolate groups, a *para*-tetrafluorophenylthiolate in **2b** and the unsubstituted phenylthiolate in **2d**. Formally, the metal centres exhibit *pseudo*-octahedral coordination geometries, being coordinated to the 6-electron donor η^5-C_5Me_5 ring and to the three bridging ligands. Although some statistically significant differences are observed for the molecular parameters collected in Table 1, most of them are chemically irrelevant, neither if compared between the different complexes **2b** or **2d**, nor between the two crystallographically independent molecules present in **2d**.

The most evident differences between both cations come from the distinct configuration of the thiolate phenyl rings relative to the bridging system (Fig. 3). While in **2d** the two phenyl rings are situated at the same side of the ideal Rh_2S_2 plane with a torsional angle C(24)–S(1) $\cdots$ S(2)–C(30) close to zero (-5.8 and 11.0(7)°), in the case of **2b** the more voluminous substituted C_6F_4H groups are disposed towards different sides of the Rh_2S_2 reference plane, showing a related torsional angle of $-177.1(5)°$. If referred to the Rh_2S_2 cyclic system, the different configurations observed could be described under the *syn–exo* (**2d**) or *anti* (**2b**) terminology.[3] The different orientation of the phenyl rings affects dramatically to the symmetry of the complexes, conforming a C_{2v} structure (**2d**) or a C_s molecule in the case of **2b**.

---

[3] In the *syn–exo* configuration, the two SR groups occupy two equatorial positions on the Rh_2S_2 ring. One axial and one equatorial substituents are present in the *anti* isomer. The third possibility, i.e., two axial substituents would be adopted in the *syn–endo* isomer (see Scheme 1).

Table 1
Selected bond lengths (Å) and angles (deg) for $[(\eta^5\text{-}C_5Me_5)_2Rh_2(\mu\text{-}Pz)(\mu\text{-}S\text{-}p\text{-}C_6F_4H)_2]BF_4$ (**2b**) and $[(\eta^5\text{-}C_5Me_5)_2(\mu\text{-}Pz)(\mu\text{-}SC_6H_5)_2]BF_4$ (**2d**)[a]

	2b	**2d**	
Rh(1) · · · Rh(2)	3.4536(10)	3.3902(6)	3.3891(8)
Rh(1)–S(1)	2.422(2)	2.397(2)	2.382(2)
Rh(2)–S(1)	2.411(2)	2.407(2)	2.389(2)
Rh(1)–S(2)	3.431(2)	2.378(2)	2.392(2)
Rh(2)–S(2)	2.418(2)	2.385(2)	2.401(2)
Rh(1)–N(1)	2.081(6)	2.067(5)	2.068(5)
Rh(2)–N(2)	2.085(6)	2.077(5)	2.065(5)
Rh(1)–G(1)[b]	1.802(4)	1.802(3)	1.799(4)
Rh(1)–G(2)	1.803(4)	1.791(3)	1.801(4)
N(1)–N(2)	1.379(7)	1.372(5)	1.364(6)
N(1)–C(1)	1.329(9)	1.328(7)	1.337(7)
N(2)–C(23)	1.351(9)	1.321(7)	1.343(7)
C(21)–C(22)	1.370(10)	1.378(8)	1.375(8)
C(22)–C(23)	1.400(10)	1.383(8)	1.353(8)
S(1)–C(24)	1.792(7)	1.799(6)	1.792(7)
S(2)–C(30)	1.774(7)	1.775(7)	1.792(6)
S(1)–Rh(1)–S(2)	81.59(7)	77.23(6)	77.44(6)
S(1)–Rh(2)–S(2)	82.09(7)	76.90(5)	77.14(6)
S(1)–Rh(1)–N(1)	87.2(2)	84.54(14)	88.24(14)
S(1)–Rh(2)–N(2)	88.3(2)	86.87(13)	86.42(14)
S(1)–Rh(1)–G(1)	131.17(11)	130.38(10)	126.35(13)
S(1)–Rh(2)–G(2)	133.26(12)	128.15(10)	128.18(13)
S(2)–Rh(1)–N(1)	76.5(2)	88.53(13)	84.1(2)
S(2)–Rh(2)–N(2)	74.7(2)	86.88(13)	86.8(2)
S(2)–Rh(1)–G(1)	128.90(11)	126.32(10)	130.84(14)
S(2)–Rh(2)–G(2)	126.16(12)	127.60(10)	127.71(13)
N(1)–Rh(1)–G(1)	132.4(2)	131.9(2)	131.9(29)
N(2)–Rh(2)–G(2)	133.5(2)	132.4(9)	132.5(2)
Rh(1)–N(1)–N(2)	119.3(5)	120.0(4)	119.8(4)
Rh(2)–N(2)–N(1)	120.2(4)	117.9(4)	118.4(5)
Rh(1)–N(1)–C(21)	132.4(5)	133.6(4)	133.6(5)
Rh(2)–N(2)–C(23)	132.1(5)	133.3(4)	133.2(4)
N(1)–N(2)–C(23)	107.5(6)	108.3(5)	108.0(5)
N(2)–N(1)–C(21)	107.3(6)	106.4(5)	106.6(5)
N(1)–C(21)–C(22)	111.7(7)	111.6(6)	110.9(6)
N(2)–C(23)–C(22)	109.4(7)	110.7(6)	110.2(6)
C(21)–C(22)–C(23)	103.9(7)	103.0(6)	104.2(6)
Rh(1)–S(1)–Rh(2)	91.23(7)	89.77(6)	90.53(5)
Rh(1)–S(2)–Rh(2)	90.81(7)	90.74(5)	90.00(6)
Rh(1)–S(1)–C(24)	114.5(2)	107.3(2)	112.3(6)
Rh(1)–S(2)–C(30)	116.8(3)	111.3(2)	107.5(2)
Rh(2)–S(1)–C(24)	113.7(2)	114.2(2)	110.6(2)
Rh(2)–S(2)–C(30)	114.2(3)	113.2(2)	114.6(2)

[a] Two independent molecules were observed in the X-ray analysis of **2d**.

[b] G(1) and G(2) represent the centroids of the two cyclopentadienyl rings present in each molecule.

The whole cationic structures closely resemble the related dinuclear complex $[(\eta^5\text{-}C_5Me_5)_2Rh_2(\mu\text{-}SC_6F_5)_3]^+$ [15], in which a bridging SC_6F_5 group has been substituted by a bidentate pyrazolate. A simple comparison of this complex with the cations of **2b** and **2d** allows a sensible explanation for the different configurations observed for **2b** and **2d**. While in the triply thiolate bridged complex $[(\eta^5\text{-}C_5Me_5)_2Rh_2(\mu\text{-}SC_6F_5)_3]^+$ the three identical bridging ligands originate the two C_5Me_5 terminal ligands to be nearly parallel (5.6(3)°), in **2b** and **2d** the greater steric requirements of the pyrazolate force the inter-planar C_5Me_5–C_5Me_5 angle to increase to values of 27.1(3)° in **2b** or 26.9(2) and 26.7(3)° in **2d**. This structural modification reduces the available space in the bridging area opposite to the pyrazolate (due to the proximity of the methyl groups C(8)–C(10) and C(17)–C(19)) and, consequently, favours a symmetric configuration with the two phenyl groups moved away from this area; that happens in the *syn–exo* geometry (**2d**). However, in the case of **2b**, the presence of *ortho* fluoro substituents in the phenyl groups would give rise in a *syn–exo* configuration to short distances between flourine atoms and the pyrazolate, destabilizing this configuration and making the *anti* geometry of lower energy. This qualitative proposal is also corroborated by the dihedral angles between the bridging planes (calculated through Rh–S(1)–Rh, Rh–S(2)–Rh and Rh–N(1)–N(2)–Rh). All the values in the C_{2v} structure **2d** are similar and close to the ideal value of 120° (range 116.0–124.0(1)°), the inter-thiolate dihedral angles being 124.0 and 124.5(1)°. In the case of the *anti* isomer **2b**, the values affecting the S(2) thiolate are altered by opening the *S(2)–S(1)* dihedral angle, 138.4(1)°, and a consequent closing of the *S(2)–Pz* one, 100.0(1)°, in a movement that allows more space for the phenyl group C(30)–C(35).

All the Rh–S bond distances are similar and reflect a barely detectable asymmetry in the bridges (see Table 1). However the mean value in **2b**, 2.421(1) Å, is slightly longer than that observed in **2d**, 2.392(1) Å. These distances compare well with those reported in the dinuclear cation $[(\eta^5\text{-}C_5Me_5)_2Rh_2(\mu\text{-}SC_6F_5)_3]^+$ (2.425(6) Å) or in the mononuclear counter anion $[(\eta^5\text{-}C_5Me_5)Rh(SC_6F_5)_3]^-$ (2.414(9) Å) of the same compound [15,16]. The bridging Rh–S–Rh angles in the homobridged complex $[(\eta^5\text{-}C_5Me_5)_2Rh_2(\mu\text{-}SC_6F_5)_3]^+$ (mean 87.0(3)°) are also comparable with values found in **2b** (91.02(3)°) and **2d** (90.26(3)°). Nevertheless, these Rh–S distances are clearly longer than those observed in related $(\eta^5\text{-}C_5Me_5)Rh^{III}$ dinuclear complexes where the bridging system contains only a double thiolate bridge, those are the cases of $[(\eta^5\text{-}C_5Me_5)Rh(\mu\text{-}L)]_2$ (L = *o*-phenylenebenzenethiolato (2.341(2) Å) and 4-methoxibuta-1-3-diene-1-thiolato (2.357(1) Å) [17]. These later complexes exhibit longer intermetallic distances (range 3.515(1)–3.565(2) Å) than those observed in **2b**, 3.4536(10) Å, or in **2d**, 3.3902(6) and 3.3891(8) Å, and as a result longer Rh–S–Rh angles (range 96.6(1)–99.5(1)°).

Within the error associated to the structural analyses, all the Rh–N bond lengths in **2b** and **2d** are statistically identical (range 2.065(5)–2.085(6) Å). These distances are comparable with those found in other dinuclear pyrazolato-bridged $(\eta^5\text{-}C_5Me_5)Rh^{III}$ complexes such as $[\{(\eta^5\text{-}C_5Me_5)Rh\}_2(\mu\text{-}Pz)(\mu\text{-}PPh_2)_2]^+$ (2.070(4) and

2.081(4) Å) [18], and $[\{(\eta^5\text{-}C_5Me_5)Rh\}_2(\mu\text{-3-Me-Pz})(\mu\text{-MeO})_2]^+$ (2.082(7) Å) [14], as well as in the related di-μ-pyrazolato complexes $[\{(\eta^5\text{-}C_5Me_5)Rh\}_2(\mu\text{-Pz})_2(\mu\text{-OH})]^+$ (average 2.092(4) Å) [14], $[\{(\eta^5\text{-}C_5Me_5)Rh\}_2(\mu\text{-Pz})_2(\mu\text{-Cl})]^+$ (*av.* 2.091(6) Å) [5] or $[\{(\eta^5\text{-}C_5Me_5)Rh\}_2(\mu\text{-Pz})_2(\mu\text{-PPh}_2)]^+$ (*av.* 2.092(2) Å) [19]. On the other hand, if we compare the separations between the metal atoms and the centroids of the C_5Me_5 rings (*avs.* 1.802(3) for **2b** and 1.798(2) Å for **2d**) with those of the latter related complexes, it seems that these Rh–C_5Me_5 centroid distances (Rh–G(1) and Rh–G(2)) are fairly sensitive to the steric requirements of the bridging ligands; that is, the shortest distances were found for $[\{(\eta^5\text{-}C_5Me_5)Rh\}_2(\mu\text{-3-Me-Pz})(\mu\text{-MeO})_2]^+$ (1.773(4) Å) [14], $[\{(\eta^5\text{-}C_5Me_5)Rh\}_2(\mu\text{-Pz})_2(\mu\text{-Cl})]^+$ (1.777(2) Å) [5] and $[\{(\eta^5\text{-}C_5Me_5)Rh\}_2(\mu\text{-Pz})_2(\mu\text{-OH})]^+$ (*av.* 1.778(2) Å) [14], intermediate separations were observed in **2b**, **2d** or in $[\{(\eta^5\text{-}C_5Me_5)Rh\}_2(\mu\text{-Pz})(\mu\text{-PPh}_2)(\mu\text{-Cl})]^+$ (*av.* 1.822(3) Å) [18], while the longest distances were determined for the phosphido-bridged complexes $[\{(\eta^5\text{-}C_5Me_5)Rh\}_2(\mu\text{-Pz})(\mu\text{-PPh}_2)_2]^+$ (*av.* 1.876(5) Å) [18] or $[\{(\eta^5\text{-}C_5Me_5)Rh\}_2(\mu\text{-Pz})_2(\mu\text{-PPh}_2)]^+$ (*av.* 1.858(2) Å) [19].

2.3. Fluxional behaviour

The dirhodium compounds **2a–d** are fluxional in the NMR time scale. Because of the different solution behaviour, we will consider separately the *ortho* and *meta* fluorine substituted thiolate derivatives **2a–b** from the *p*-substituted and unsubstituted thiolate **2c**–**d** compounds.

2.3.1. Penta- and tetra-fluorophenyl thiolate complexes *2a* and *2b*

The room temperature ^1H NMR spectrum of compound **2a**, in CD_2Cl_2, consists of one singlet at 1.44 ppm due to the C_5Me_5 groups and one triplet and one doublet centred at 6.47 and 7.45 ppm, respectively, assigned to the protons of the pyrazolate group. The spectrum is essentially invariant over all the range of temperature investigated. Only small changes in the chemical shifts and in the resolution of the doublet and triplet pyrazolate signals have been observed. However, variable temperature ^{19}F NMR studies show that the complex is fluxional. At −110°C, in CD_2Cl_2, the ^{19}F NMR spectrum of compound **2a** consists of ten well resolved multiplets, one for each fluorine nucleus of the molecule, along with the BF_4 resonance. This low-temperature-limiting spectrum is compatible with a static *anti* structure with the planes of the phenyl groups of the thiolate ligands being perpendicular to the Rh–Rh vector (see Scheme 1). In fact, the related derivative $[(\eta^5\text{-}C_5Me_5)_2Rh_2(\mu\text{-Pz})(\mu\text{-S-}p\text{-}C_6F_4H)_2]BF_4$ (**2b**), with the tetra-substituted S-*p*-C_6F_4H ligand, presents an

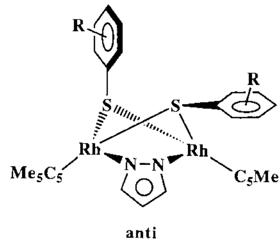

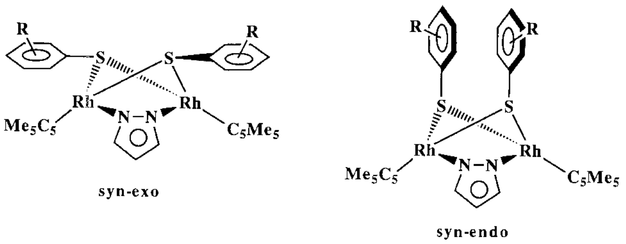

Scheme 1.

anti disposition for the two thiolate groups and the angles between the two substituted phenyl rings and their respective Rh–S–Rh planes are 71.3(2) (S(1)) and 89.5(2)° (S(2)). On warming, from −110 to −55°C, while the two F_{ortho} signals at −129.3 and −135.9 ppm and the two F_{meta} signals at −159.4 and −160.3 ppm broadened and coalesced, the other two F_{ortho} and F_{meta} resonances as well as the two F_{para} signals remained unchanged (the evolution of the F_{ortho} signals is collected in Scheme 2). The rotation of one of the two thiolate rings around its C–S bond would explain the observed spectra: the *ortho* and *meta* fluorine nuclei equilibrate while the *para* fluorine remains unaltered. Relying on the static intramolecular interatomic distances, obtained in the X-ray structure of **2b**, between *ortho* fluorine atoms and hydrogens of the C_5Me_5 groups, it seems sensible to assume that the equatorial phenyl ring (labelled C(24)–C(29)) is comparatively less hindered by the C_5Me_5 ligand to rotate along the C(24)–S(1) bond and, consequently, to make equivalent both *ortho*- and *meta*-fluorines of this phenyl group. [4] The F_{ortho} signals coalesce at −55°C and from this equilibration the free energy of activation $\Delta G^{\ddagger}$ at the coalescence temperature for the rotation process has been calculated as 37.7 kJ mol^{-1}. Above −55°C two new processes become important. One of them implies the equilibration of the two additional F_{ortho} and F_{meta} and, interestingly, the other produces the equilibration between the two F_{para}. At the highest temperature measured, +80°C in a 1/1 v/v mixture of $CDCl_3$ and toluene-d^8, the spectrum only shows three signals, one

---

[4] In the case of the axial C_6F_4H group the F(31) atom exhibits short F···H (C_5Me_5) interatomic distances (close to the limit of the sum of the van der Waals radii, 2.56 Å) with *both* C_5Me_5 groups (F(31)···H(9c) 2.65(3) and F(31)···H(18c) 2.59(4) Å).

for each type of *ortho*, *meta*, and *para* fluorine atoms. Consequently, we propose that the two new processes consisted of the rotation of the second thiolate ring around its C–S bond (C(30)–S(2)) and the isomerization of the *anti* isomer to one or to the two possible *syn* isomers depicted in Scheme 1 as *syn–exo* and *syn–endo*. For the isomerization process it is possible to calculate a $\Delta G^{\ddagger}$ value of 53.9 kJ mol^{-1} at the coalescence temperature from the equilibration of the two F_{para}. This process could involve cleavage of one of the Rh–S–Rh bridges, rotation about the resulting terminal Rh–S bond, and regeneration of the Rh_2S_2 ring.

The fluxional behaviour of the tetrafluorophenyl derivative **2b** is essentially similar to that described for the pentafluorophenyl thiolate **2a**. At −110°C, in CD_2Cl_2, the ^1H NMR spectrum shows, along with the pentamethylcyclopentadienyl and pyrazolate resonances, two *pseudo*quintets centred at 7.11 and 7.38 ppm attributed to the two protons of the *para* position of the two inequivalent thiolate ligands. The ^{19}F NMR spectrum, at the same temperature, besides the BF_4 resonance, consists of four F_{ortho} and four F_{meta} resonances. These spectra are the expected for a structure with an *anti* disposition of the two thiolate ligands as that found in the diffractometric analysis reported above. Thus, at low temperature, in solution, the compound retains the solid structure. However, on warming, two of the F_{ortho} resonances coalesced at −55°C. The calculated $\Delta G^{\ddagger}$ value for the rotation process was 37.4 kJ mol^{-1}. From the equilibration of the two H_{para} ($t_{coalescence} = 0$°C) we obtain a $\Delta G^{\ddagger}$ value of 54.9 kJ mol^{-1} for the isomerization process. Both $\Delta G^{\ddagger}$ values are comparable to the above reported for **2a** supporting that the fluxional processes involved would be also similar.

2.3.2. *p-fluorophenyl and phenyl thiolate complexes **2c** and **2d***

The ^1H and ^{19}F NMR spectra, in CD_2Cl_2, of the *p*-fluorophenyl thiolate complex **2c** show the presence of three isomers in a relative proportion of ca. 70, 28, and 2%, at −60°C. The major isomer only contain one type of phenyl thiolate ring and we assume that it is the *syn–exo* isomer depicted in Scheme 1 on the basis of the crystal structure determination carried out on the related phenyl thiolate complex **2d** and on the steric

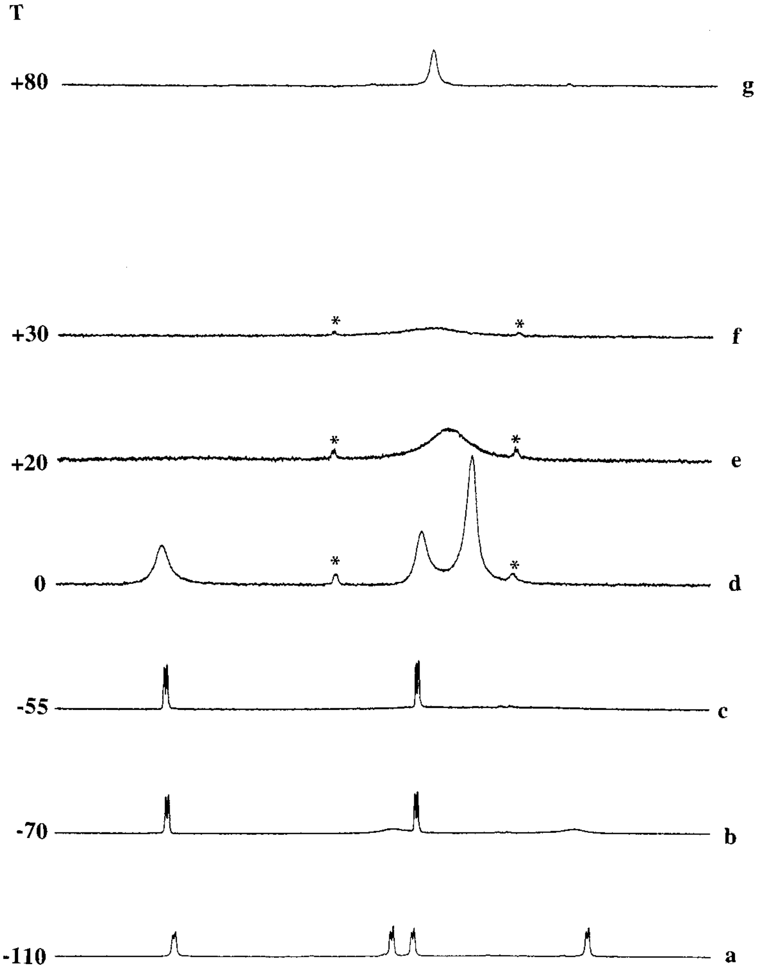

Scheme 2. F_{ortho} resonances region of the spectra of $[(\eta^5\text{-}C_5Me_5)_2Rh_2(\mu\text{-}Pz)(\mu\text{-}SC_6F_5)_2]BF_4$ (**2a**) in CD_2Cl_2 (a–f) or in $CDCl_3$/toluene-d^8, 1/1, v/v (g) at selected temperatures (°C). The asterisks denote an impurity.

arguments described along the structural discussion (see above). There are two types of thiolate rings in the 28% abundant isomer and, consequently, it is the *anti* isomer. The 2% of the mixture should be the *syn–endo* isomer in which the two thiolate ligands are also equivalent both occupying axial positions in the Rh_2S_2 ring. Additionally, the ^1H NMR spectrum at −70°C shows an unique type of *ortho* and *meta* protons for the two *syn* isomers and only two types of this kind of protons for the *anti* isomer. Thus, even at −70°C, the thiolates of the three isomers are rapidly rotating about their C–S bond. By diminishing the temperature, all the resonances slowly broaden but, only the *ortho* protons of the major isomer achieved the coalescence temperature at −130°C, the lowest temperature of measurement ($CD_2Cl_2/CFCl_3$, 1/1, v/v as solvent). Thus, the rotation is operating even at −130°C for the three isomers. From −70 to −10°C sharp and well resolved resonances are observed in both proton and ^{19}F spectra but, above the later temperature, the equilibration between the *anti* and *syn–exo* isomers was observed. From the coalescence temperature of the two C_5Me_5 singlets (+35°C) a value of 64.9 kJ mol^{-1} was calculated for the activation energy for this isomerization. Interestingly, the signals attributed to the *syn–endo* isomer remained sharp to +50°C. Only above this temperature its participation into the exchange process becomes apparent. These proposals are strongly supported by the evolution of the ^{19}F NMR spectra with temperature which follows completely compatible trends with the proton NMR behaviour.

The fluxional behaviour of the phenyl derivative **2d** is similar to that described for the *p*-fluorophenyl thiolate **2c**. The X-ray molecular structure determination of **2d** establish the presence in the solid state of the *syn–exo* isomer (see Fig. 2 and Scheme 1). However, the ^1H NMR spectra recorded from −130 to +90°C reveal the presence of three isomers that we assign to the *syn–exo*, *anti*, and *syn–endo* isomers depicted in Scheme 1. At −50°C the relative amount of each isomer was ca. 59, 34 and 7%, respectively. We assume that the major component is the *syn–exo* isomer instead of the *syn–endo* on the basis of the X-ray crystal structure determination. As in the *p*-fluorophenyl thiolate case, the rotation of the thiolate rings operates in all the range of temperature investigated and above +10°C the conversion between the *syn–exo* and *anti* isomers takes place. The two C_5Me_5 singlets coalesced at +45°C the corresponding $\Delta G^{\ddagger}$ value being 66.8 kJ mol^{-1}.

3. Conclusions

The presence of fluorine substituents on the *ortho* and *meta* positions of the thiolate rings strongly affects the solution and solid state properties of the dirhodium compounds **2a–d**. Thus, while, at low temperatures, the *anti* isomer was the sole species observed for the perfluoro **2a** and the tetrafluoro **2b** derivatives, mixtures of the three possible isomers were detected for the *p*-fluorine substituted **2c** or the unsubstituted **2d** compounds, the *syn–exo* isomer being the major component. Moreover, solid **2b** has the *anti* disposition whereas the *syn–exo* isomer was found in solid **2d** in the crystallographic analyses carried out. The four complexes undergo fluxional processes observable by NMR. Excluding the Rh_2S_2 ring inversion, precluded by the presence of the bridging pyrazolate ligand, two movements could be envisaged as responsible for the dynamic behaviour observed: rotation around the C–S thiolate bond and isomerization. As expected, the first is less energetically demanding for the *ortho* and *meta* unsubstituted compounds **2c–d** than for the tetra or pentafluoro thiolato derivatives **2a–b**. Furthermore, the rotation of the equatorial thiolate rings of the *anti* isomers of complexes **2a** and **2b**, was more easily achieved than that of the axial ones as indicated by the geometrical parameters determined in the structural analyses. The rotation of the axial groups was observed by NMR at the same range of temperatures than the isomerization process. In the latter, at low temperatures, only the *anti* and *syn–exo* isomers were involved but at higher energies also the *syn–endo* isomer was concerned. Finally, from coalescence phenomena, the calculated values of the energy of activation for the *syn–exo–anti* isomerization process were greater by ca. 16 kJ mol^{-1} than that of the rotation of the equatorial thiolate rings.

4. Experimental details

All operations were carried out under inert atmosphere (high purity argon) using standard Schlenk techniques. Infrared spectra were recorded on Nicolet 550 and Perkin-Elmer 1615 FT-IR spectrophotometers. Carbon, hydrogen, and nitrogen analyses were performed using a Perkin-Elmer 2400 microanalyzer. NMR spectra were recorded on either a Varian UNITY 300 or a Bruker AXR spectrometer using $SiMe_4$ (^1H, ^{13}C) or $CFCl_3$ (^{19}F) as external standards. Chemical shifts are expressed in ppm upfield from $SiMe_4$ (^1H, ^{13}C) or $CFCl_3$ (^{19}F). Coupling constants *J* are given in Hertz. The variable temperature experiments were measured from −130°C to −110°C in $CD_2Cl_2/CFCl_3$, 1/1, v/v, from −110 to +40°C in CD_2Cl_2 and from +40 to +90°C in $CDCl_3$/toluene-d^8, 1/1, v/v. Mass spectra were measured on a VG Autospec double-focusing mass spectrometer operating in the FAB^+ mode. Ions were produced with the standard Cs^+ gun at ca. 30 kV, and 3-nitrobenzyl alcohol (NBA) was used as matrix.

The compound $[(\eta^5\text{-}C_5Me_5)_2Rh_2(\mu\text{-}Pz)_2(\mu\text{-}OH)]BF_4$ (**1**) was prepared as previously described [14]. The fluorothiophenols and thiophenol were obtained from Aldrich, and used as received.

4.1. $[(\eta^5\text{-}C_5Me_5)_2Rh_2(\mu\text{-}Pz)(\mu\text{-}SC_6F_5)_2]BF_4$ (**2a**)

The ligand HSC_6F_5 (pentafluorothiophenol) (0.392 mmol, 78.5 mg, 60 μl) was added to a solution of complex $[(\eta^5\text{-}C_5Me_5)_2Rh_2(\mu\text{-}Pz)_2(\mu\text{-}OH)]BF_4$ (**1**) (140 mg, 0.196 mmol) in dichloromethane (10 ml) giving an orange–reddish solution, which was stirred (25°C, 75 min). The reaction mixture was evaporated in vacuo, giving an orange residue which was chromatographed on a silica gel-60 (70–230 mesh) column. Elution with dichloromethane gave a deep green fraction which, when dried gave a purple–brownish solid (identified as $[(\eta^5\text{-}C_5Me_5)_2Rh_2(\mu\text{-}SC_6F_5)_3][(\eta^5\text{-}C_5Me_5)Rh(SC_6F_5)_3]$, see Ref. [15,16]). When eluting with dichloromethane:acetone (4:1), an orange fraction was obtained and, after drying, it gave a reddish solid **2a** (188 mg, 0.183 mmol, 93%). Anal. Found: C, 40.95; H, 3.2; N, 2.9; S, 6.0%. $C_{35}H_{33}BF_{14}N_2Rh_2S_2$ requires C, 40.9; H, 3.2; N, 2.8; S, 6.2%. NMR: ^1H ($CDCl_3$, RT, δ) 1.44 (s, 30H, C_5Me_5), 6.47 (t, ^3J (HH) 2.5, 1H, Pz), 7.74 (d, 2H, Pz); ^{19}F (CD_2Cl_2, −110°C, δ) −121.97, −129.28, −130.00, −135.86 (m, *o*-F), −149.38, −151.74 (m, *p*-F), −158.56, −158.92, −159.44, −160.31 (m, *m*-F), −151.95 (m, BF_4); ^{13}C (CD_2Cl_2, +40°C, δ) 8.95 (s, $C_5\mathit{Me}_5$), 98.24 (d, J(RhC) 7.4, C_5Me_5), 108.64 (s, C_4 Pz), 139.97 (s, C_3 and C_5 Pz) 108.21 (t, J(RhC) 19.6, C_{ipso}) 136–152 (*o,m,p*-thiolate carbons). MS (FAB^+): m/z 941 (M^+, 100), 741 (M^+–SC_6F_5, 8), 437 ($C_5Me_5RhSC_6F_5$, 10), 305 (C_5Me_5RhPz, 68), 237 (C_5Me_5Rh, 44).

4.2. $[(\eta^5\text{-}C_5Me_5)_2Rh_2(\mu\text{-}Pz)(\mu\text{-}S\text{-}p\text{-}C_6F_4H)_2]BF_4$ (**2b**)

This complex was prepared analogously to **2a**, from **1** (130 mg, 0.182 mmol), with the addition of HSC_6F_4H (2,3,5,6-tetrafluorothiophenol) (0.364 mmol, 66.3 mg, 50 μl.). When eluting the reaction mixture on a silica gel column, the first fraction (green), was obtained in a rather small amount than that of **2a** and the main fraction (orange) eluted with dichloromethane:acetone (6:1). After drying it an orange–reddish solid **2b** (146 mg, 0.147 mmol, 81%) was obtained. Anal. Found: C, 42.5; H, 3.3; N, 2.9; S, 6.45%. $C_{35}H_{35}BF_{12}N_2Rh_2S_2$ requires C, 42.4; H, 3.55; N, 2.8; S, 6.5%. NMR: ^1H (CD_2Cl_2, −70°C, δ) 1.41 (s, 30H, C_5Me_5), 6.56 (t, ^3J(HH) 2.1, 1H, Pz), 7.11 (sq, J 7.4, 1H, *p*-H SC_6F_4H), 7.37 (sq, J 7.6, 1H, *p*-H SC_6F_4H), 7.80 (d, 2H, Pz); ^{19}F (CD_2Cl_2, −110°C, δ) −121.56, −129.12, −130.20, −137.17 (m, *o*-F), −135.53, −135.80, −135.92, (m, *m*-F), −150.47 (m, BF_4). MS (FAB^+): m/z 905 (M^+, 100), 723 (M^+–SC_6F_4H, 9), 419 ($C_5Me_5RhSC_6F_4H$, 7), 305 (C_5Me_5RhPz, 35), 237 (C_5Me_5Rh, 20).

4.3. $[(\eta^5\text{-}C_5Me_5)_2Rh_2(\mu\text{-}Pz)(\mu\text{-}S\text{-}p\text{-}C_6H_4F)_2]BF_4$ (**2c**)

This complex was obtained analogously from **1** (120 mg, 0.168 mmol) with the addition of HSC_6H_4F (*p*-fluorothiophenol) (0.336 mmol, 43.1 mg, 30 μl). In this case when eluting the reaction mixture, a pretty small amount of the green by-product was obtained and the main fraction (orange) eluted with dichloromethane:acetone (8:1); on drying it an orange solid **2c** (112 mg, 0.127 mmol, 74%) was obtained. Anal. Found: C, 47.3; H, 4.8; N, 3.0; S, 7.3%. $C_{35}H_{41}BF_6N_2Rh_2S_2$ requires C, 47.5; H, 4.7.; N, 3.2; S, 7.25%. NMR: ^1H (CD_2Cl_2, −60°C, δ) *syn–exo* isomer: 1.42 (s, 30H, C_5Me_5), 6.59 (t, ^3J (HH) 2.1, 1H, Pz), 6.31 (m, 4H, *o*-H SC_6H_4F), 6.76 (m, 4H, *m*-H SC_6H_4F) 7.70 (d, 2H, Pz); *anti* isomer: 1.33 (s, 30H, C_5Me_5), 6.58 (t, 1H, Pz), 7.00 (m, 2H *o*-H SC_6H_4F), 7.20 (m, 2H *o*-H SC_6H_4F), 7.56 (m, 2H, *m*-H SC_6H_4F), 7.73 (m, 2H, *m*-H SC_6H_4F), 7.76 (d, 2H, Pz); *syn–endo* isomer: 1.28 (s, 30H, C_5Me_5), 7.07 (m, *m*-H SC_6H_4F). ^{19}F (CD_2Cl_2, −60°C, δ) *syn–exo* isomer: −113.70 m; *anti* isomer −111.58 m, −113.53 m; *syn–endo* isomer: −113.22 m. MS (FAB^+): m/z 797 (M^+, 100), 669 (M^+–SC_6H_4F, 9), 365 ($C_5Me_5RhSC_6H_4F$, 18), 305 (C_5Me_5RhPz, 8), 237 (C_5Me_5Rh, 20).

4.4. $[(\eta^5\text{-}C_5Me_5)_2Rh_2(\mu\text{-}Pz)(\mu\text{-}SC_6H_5)_2]BF_4$ (**2d**)

This complex was prepared analogously from **1** (130 mg, 0.182 mmol) with the addition of HSC_6H_5 (thiophenol) (0.364 mmol, 40.1 mg, 35 μl). The main fraction (orange) was eluted with dichloromethane:acetone (10:1) and, on drying it, an orange solid **2d** (144 mg, 0.169 mmol, 92%) was obtained. Anal. Found: C, 49.5; H, 5.25; N, 3.2%. $C_{35}H_{43}BF_4N_2Rh_2S_2$ requires: C, 49.55; H, 5.1; N, 3.3%). NMR: ^1H (CD_2Cl_2, −50°C, δ) *syn–exo* isomer: 1.42 (s, 30H, C_5Me_5), 6.39 (d, J 7.6, 4H, *o*-H SC_6H_5), 6.595 (t, ^3J (HH) 2.1, 1H, Pz), 7.03 (st, 4H, *m*-H SC_6H_5), 7.18 (st, 2H, *p*-H SC_6H_5), 7.70 (d, 2H, Pz); *anti* isomer: 1.32 (s, 30H, C_5Me_5), 6.34 (d, J 7.6, 4H, *o*-H SC_6H_5), 6.59 (t, ^3J (HH) 2.1, 1H, Pz), 7.77 (d, 2H, Pz); *syn–endo* isomer: 1.28 (s, 30H, C_5Me_5). MS (FAB^+): m/z 761 (M^+, 100), 652 (M^+–SC_6H_5, 7), 347 ($C_5Me_5RhSC_6H_5$, 15), 237 (C_5Me_5Rh, 11).

4.5. X-ray structure determination of $[(\eta^5\text{-}C_5Me_5)_2Rh_2(\mu\text{-}Pz)(\mu\text{-}S\text{-}p\text{-}C_6F_4H)_2]BF_4$ (**2b**) and $[(\eta^5\text{-}C_5Me_5)_2Rh_2(\mu\text{-}Pz)(\mu\text{-}SC_6H_5)_2]BF_4$ (**2d**)

4.5.1. Crystal data for **2b**

$C_{35}H_{35}BF_{12}N_2Rh_2S_2$; $M = 992.40$; monoclinic, space group $P2_1/n$; $a = 14.368(2)$, $b = 18.252(2)$, $c = 15.268(2)$ Å, $\beta = 109.79(1)°$, $V = 3767.4(8)$ Å^3, $Z = 4$;

$D_c = 1.750$ Mg m^{-3}; $F(000) = 1976$; λ(Mo–K$_\alpha$) = 0.71073 Å; $\mu = 1.076$ mm^{-1}; $T = 150.0(2)$ K.

4.5.2. Crystal data for **2d**

$C_{35}H_{43}BF_4N_2Rh_2S_2$; $M = 848.47$; monoclinic, space group $C2/c$; $a = 48.723(5)$, $b = 8.7503(8)$, $c = 40.334(4)$ Å, $\beta = 122.620(5)°$, $V = 14484(3)$ Å^3, $Z = 16$; $D_c = 1.556$ Mg m^{-3}; $F(000) = 6880$; λ(Mo–K$_\alpha$) = 0.71073 Å; $\mu = 1.074$ mm^{-1}; $T = 293$ K.

Table 2
Selected atomic co-ordinates[a] ($\times 10^4$) and equivalent isotropic displacement parameters (Å$^2 \times 10^3$) for the complex $[(\eta^5\text{-}C_5Me_5)_2Rh_2(\mu\text{-Pz})(\mu\text{-S-}p\text{-}C_6F_4H)_2]BF_4$ (**2b**)

	x	y	z	U_{eq}[b]
Rh(1)	5829.7(4)	− 1950.8(4)	6295.7(4)	24.1(2)
Rh(2)	3483.2(4)	− 1912.9(4)	6441.1(4)	25.7(2)
S(1)	5120(1)	− 1601(1)	7465(1)	25.9(5)
S(2)	4401(1)	− 2760(1)	5825(1)	26.6(5)
N(1)	4734(4)	− 1318(3)	5359(4)	29(2)
N(2)	3784(4)	− 1341(3)	5385(4)	24(2)
C(1)	6831(5)	− 2384(4)	5654(5)	25(2)
C(2)	7097(5)	− 1640(4)	5869(5)	29(2)
C(3)	7340(5)	− 1541(40	6848(6)	28(2)
C(4)	7287(5)	− 2248(4)	7249(5)	28(2)
C(5)	6979(6)	− 2762(4)	6518(6)	29(2)
C(6)	6548(6)	− 2725(4)	4709(6)	41(2)
C(7)	7204(5)	− 1069(4)	5211(5)	38(2)
C(8)	7734(6)	− 864(4)	7397(5)	42(2)
C(90	7605(5)	− 2402(5)	8268(5)	38(2)
C(10)	6962(6)	− 3568(4)	6634(6)	45(2)
C(11)	1891(5)	− 2073(5)	5956(5)	32(2)
C(12)	2372(6)	− 2653(40	6591(6)	31(2)
C(13)	2882(5)	− 2335(5)	7460(6)	31(2)
C(14)	2713(6)	− 1558(5)	7373(6)	36(2)
C(15)	2118(5)	− 1411(5)	6460(6)	35(2)
C(16)	1199(5)	− 2187(5)	4974(5)	49(3)
C(17)	2229(6)	− 3447(5)	6383(7)	48(3)
C(18)	3391(6)	− 2724(5)	8344(6)	52(3)
C(19)	3023(6)	− 1007(5)	8153(6)	51(3)
C(20)	1690(6)	− 665(5)	6077(6)	49(2)
C(21)	4700(6)	− 95794)	4594(5)	34(2)
C(22)	3764(6)	− 714(4)	4113(5)	36(2)
C(23)	3192(5)	− 998(4)	4622(5)	31(2)
C(24)	5265(5)	− 652(4)	7783(5)	22(2)
C(25)	4719(6)	− 71(4)	7311(5)	29(2)
F(25)	3994(3)	− 164(2)	6487(3)	51(1)
C(26)	4857(7)	622(5)	7673(6)	40(2)
F(26)	4249(4)	1159(2)	7160(30)	55(2)
C(27)	5547(6)	790(5)	8517(6)	41(2)
C(28)	6082(6)	223(5)	8977(6)	45(2)
F(28)	6820(4)	344(3)	9815(3)	70(2)
C(29)	5969(6)	− 472(4)	8617(5)	38(2)
F(29)	6563(30	− 1012(3)	9152(3)	54(1)
C(30)	4559(5)	− 3641(4)	6345(5)	23(2)
C(310	4969(6)	− 3775(4)	7283(5)	31(2)
F(31)	5320(3)	− 3220(2)	7882(3)	39(1)
C(32)	5055(6)	− 4478(5)	7633(6)	53(2)
F(320	5465(4)	− 4570(5)	8566(3)	54(1)
C(33)	4744(6)	− 5066(4)	7069(6)	42(2)
C(34)	4343(6)	− 4934(5)	6133(6)	42(2)
F(34)	4035(4)	− 5509(3)	5533(4)	70(2)
C(35)	4260(6)	− 4248(4)	5769(6)	34(2)
F(35)	3861(3)	− 4158(2)	4841(3)	53(1)

[a] The atomic co-ordinates of the disordered anions have been omitted.
[b] U_{eq} is defined as one third of the trace of the orthogonalized $\mathbf{U}_{ij}$ tensor.

4.5.3. Data collection and processing

Suitable crystals for the X-ray determinations were grown by slow diffusion of hexane into ethanolic solutions of complexes **2b** and **2d**. An orange irregular plate of approximate dimensions 0.25 × 0.15 × 0.06 mm was used in the analysis of **2b**; a yellow–orange prismatic block, 0.38 × 0.18 × 0.12 mm, in the case of **2d**. Intensity data were collected on a Siemens-P4 diffractometer using graphite monochromated Mo–K$_\alpha$ radiation. Cell parameters were determined by least-squares refinement from the 2θ values of 58 (**2b**) or 52 (**2d**) accurately centred reflections ($20 \leq 2\theta \leq 30°$). A conventional $\omega/2\theta$ scan mode was applied for the measurement of data in **2b**, whereas the long length of two cell parameters in **2d** suggested a ω-scan to be more appropriate. A total of 5950 (**2b**) or 11323 reflections (**2d**) ($4 \leq 2\theta \leq 45°$) were collected; 4862 independent reflections ($R_{int} = 0.059$) in **2b** and 9383 for complex **2d** ($R_{int} = 0.029$) were used in the analyses. A set of three standard reflections were monitored along both data collections as a check of crystal and instrument stability. The weak intensity decay observed along data collection of **2b** (2.4%) was amended according to standard reflections. Data were corrected for Lorentz and polarization effects. A semiempirical correction for absorption, via ψ-scans, was also applied (max. and min. trans. fact. 0.878 and 0.809 for **2b**; 0.891 and 0.837 for **2d**) [20].

4.5.4. Structure solution and refinement

The structures were solved by direct and Fourier methods (SIR92 [21]) and refined by full-matrix least-squares (SHELXL-93 [22]). Atoms were refined isotropically first, and in subsequent cycles with anisotropic thermal parameters for all the non-hydrogen atoms. C_5Me_5 hydrogen atoms in **2b** were included in calculated positions, but those of the bridging ligands were found from different Fourier maps; all hydrogens in this molecule were refined riding on their respective carbon atoms with two common thermal parameters (one for C_5Me_5 and one for bridging groups). In the case of **2d**, all the hydrogens were included in calculated positions and were refined in a similar way to that described for **2b**. In both structures, the BF_4^- anions exhibit static disorder. Each independent anion was modeled on the basis of two BF_4^- groups with restricted interatomic distances and complementary occupancy factors. A weighting scheme was used in the final steps of the refinements: $w^{-1} = [\sigma^2(F_o)^2 + (aP)^2]$ where $P = (F_o^2 + 2F_c^2)/3$ with $a = 0.0313$ (**2b**) and 0.0135 (**2d**). Refinements converged to $R(F) = 0.0401$ (for 2865 observed reflections, $I \geq 2\sigma(I)$) and $wR(F^2) = 0.0876$ for **2b**, and $R(F) = 0.0337$ (5328 observed reflections,

Table 3
Selected atomic co-ordinates[a] ($\times 10^4$) and equivalent isotropic displacement parameters ($Å^2 \times 10^3$) for the two independent molecules of the complex $[(\eta^5\text{-}C_5Me_5)_2Rh_2(\mu\text{-Pz})(\mu\text{-}SC_6H_5)_2]BF_4$ (**2d**)

	x	*y*	*z*	U_{eq}^{b}
Rh(1)	3939.3(1)	−709.7(6)	8391.5(1)	33.0(1)
Rh(2)	3544.8(1)	−1127.4(6)	7401.7(1)	32.5(1)
S(1)	3531(1)	−2420(2)	7919(1)	35.4(4)
S(2)	4101(1)	−1084(2)	7936(1)	36.9(4)
N(1)	3626(1)	986(6)	8027(1)	35(1)
N(2)	3487(1)	893(6)	7628(1)	35(1)
C(1)	4208(2)	524(9)	8943(2)	51(2)
C(2)	3975(2)	−446(11)	8948(2)	58(2)
C(3)	4052(2)	−1976(10)	8916(2)	60(2)
C(4)	4325(2)	−1961(10)	8882(2)	55(2)
C(5)	4428(2)	−406(9)	8909(2)	47(2)
C(6)	4247(2)	2219(9)	9007(2)	100(3)
C(7)	3703(2)	27(10)	9001(2)	106(4)
C(8)	3886(2)	−3340(9)	8951(2)	115(4)
C(9)	4492(2)	−3356(9)	8860(2)	102(3)
C(10)	4729(1)	88(9)	8924(2)	86(3)
C(11)	3420(2)	−486(8)	6815(2)	39(2)
C(12)	3652(2)	−1684(8)	6960(2)	45(2)
C(13)	3525(2)	−2975(8)	7046(2)	49(2)
C(14)	3198(2)	−2601(8)	6927(2)	46(2)
C(15)	3132(2)	−1093(8)	6794(2)	42(2)
C(16)	3454(2)	1059(7)	6685(2)	56(2)
C(17)	3978(2)	−1586(8)	7006(2)	65(2)
C(18)	3688(2)	−4499(8)	7189(2)	88(3)
C(19)	2964(2)	−3676(8)	6943(2)	72(2)
C(20)	2810(1)	−306(7)	6621(2)	61(2)
C(21)	3520(2)	2282(8)	8092(2)	53(2)
C(22)	3316(2)	3061(8)	7746(2)	64(2)
C(23)	3309(2)	2131(7)	7464(2)	43(2)
C(24)	3165(1)	−2083(8)	7917(2)	38(2)
C(25)	2962(2)	−850(9)	7744(2)	65(2)
C(26)	2701(2)	−669(10)	7784(2)	84(3)
C(27)	2637(2)	−1672(11)	7981(2)	83(3)
C(28)	2832(2)	−2905(10)	8149(2)	79(3)
C(29)	3090(2)	−3142(8)	8109(2)	60(2)
C(30)	4319(2)	519(9)	7925(2)	43(2)
C(31)	4587(2)	187(9)	7901(2)	59(2)
C(32)	4778(2)	1366(11)	7909(2)	76(3)
C(33)	4713(2)	2849(11)	7932(2)	81(3)
C(34)	4443(2)	3177(9)	7954(2)	75(3)
C(35)	4245(2)	2016(9)	7946(2)	54(2)
Rh(51)	34044(1)	−40343(7)	53685(1)	361(2)
Rh(52)	41589(1)	−36927(6)	55263(1)	351(2)
S(51)	3941(1)	−3744(2)	5934(1)	412(5)
S(52)	3652(1)	−2347(2)	5137(1)	376(5)
N(51)	3582(1)	−5733(6)	5177(1)	39(1)
N(52)	3897(1)	−5672(6)	5274(1)	39(1)
C(51)	2879(1)	−4245(9)	5011(2)	46(2)
C(52)	3001(2)	−5245(9)	5341(2)	47(2)
C(53)	3164(2)	−4331(10)	5684(2)	49(2)
C(54)	3147(2)	−2801(9)	5576(2)	45(2)
C(55)	2960(2)	−2720(9)	5161(2)	45(2)
C(56)	2673(1)	−4656(9)	4578(2)	81(3)
C(57)	2953(2)	−6930(9)	5328(2)	81(3)
C(58)	3312(2)	−4915(8)	6098(2)	77(3)
C(59)	3269(1)	−1444(8)	5852(2)	71(2)
C(60)	2858(1)	−1272(9)	4922(2)	72(2)
C(61)	4521(1)	−3736(10)	5367(2)	50(2)
C(62)	4435(2)	−2192(9)	5380(2)	54(2)
C(63)	4510(2)	−1891(8)	5765(2)	50(2)
C(64)	4660(2)	−3206(10)	6000(2)	50(2)
C(65)	4661(1)	−4381(8)	5759(2)	43(2)
C(66)	4499(2)	−4471(9)	5017(2)	95(3)
C(67)	4296(2)	−1049(9)	5052(2)	100(3)
C(68)	4469(2)	−386(8)	5916(2)	101(3)
C(69)	4814(1)	−3374(9)	6434(2)	89(3)
C(70)	4802(2)	−5948(8)	5886(2)	84(3)
C(71)	3453(2)	−7005(8)	4965(2)	57(2)
C(72)	3680(2)	−7807(8)	4934(2)	63(2)
C(73)	3956(2)	−6939(8)	5134(2)	52(2)
C(74)	4077(2)	−5413(9)	6239(2)	48(2)
C(75)	3990(2)	−6893(9)	6106(2)	62(2)
C(76)	4109(2)	−8087(10)	6371(3)	80(3)
C(77)	4318(2)	−7841(11)	6762(3)	87(4)
C(78)	4400(2)	−6387(12)	6891(2)	85(3)
C(79)	4289(2)	−5149(9)	6644(2)	58(2)
C(80)	3452(1)	−2631(8)	4617(2)	41(2)
C(81)	3228(1)	−1510(8)	4372(2)	45(2)
C(82)	3055(2)	−1698(10)	3967(2)	63(2)
C(83)	3101(2)	−2963(10)	3807(2)	71(3)
C(84)	3320(2)	−4054(10)	4041(2)	76(3)
C(85)	3500(2)	−3888(9)	4449(2)	61(2)

[a] The atomic co-ordinates of the disordered anions have been omitted.
[b] U_{eq} is defined as one third of the trace of the orthogonalized $\mathbf{U}_{ij}$ tensor.

$I \geq 2\sigma(I)$) and $wR(F^2) = 0.0520$ for **2d** [22]. Atomic scattering factors, corrected for anomalous dispersion, were taken from Ref. [23]. Final atomic coordinates are given in Tables 2 and 3. Additional material available from the Cambridge Crystallographic Data Center comprises H-atom coordinates, thermal parameters and remaining bond lengths and angles (CIF file).

Acknowledgements

We thank CONACYT (México) and Consejo Superior de Investigaciones Científicas (Spain) for financial support.

References

[1] P.M. Maitlis, Accounts Chem. Res. 11 (1978) 301.
[2] P.M. Maitlis, Chem. Soc. Rev. 10 (1981) 1.
[3] C. Tejel, M.A. Ciriano, A.J. Edwards, F.J. Lahoz, L.A. Oro, Organometallics 16 (1997) 45.
[4] C. Tejel, J.M. Villoro, M.A. Ciriano, J.A. López, E. Eguizábal, F.J. Lahoz, V.I. Bakhmutov, L.A. Oro, Organometallics 15 (1996) 2967, and references therein.
[5] J.A. Bailey, S.L. Grundy, S.R. Stobart, Organometallics 9 (1990) 536, and references therein.
[6] X. He, A. Maisonnat, F. Dahan, R. Poilblanc, Organometallics 10 (1991) 2443, and references therein.
[7] M.T. Pinillos, A. Elduque, J.A. López, F.J. Lahoz, L.A. Oro, J. Chem. Soc., Dalton Trans. (1991) 1391 and references therein.
[8] L.A. Oro, D. Carmona, M. Esteban, Trends in organometallic chemistry, Trivandrum, India 1 (1994) 565, and references therein.

[9] D. Carmona, M.P. Lamata, J. Ferrer, J. Modrego, M. Perales, F.J. Lahoz, R. Atencio, L.A. Oro, J. Chem. Soc., Chem Commun. (1994) 575.
[10] D. Carmona, L.A. Oro, M.P. Lamata, M.L. Jimeno, J. Elguero, A. Belguise, Ph. Lux, Inorg. Chem. 33 (1994) 2196.
[11] D. Carmona, F.J. Lahoz, R. Atencio, A.J. Edwards, L.A. Oro, M.P. Lamata, M. Esteban, S. Trofimenko, Inorg. Chem. 35 (1996) 2549.
[12] J.J. García, M.L. Hernández, H. Torrens, A. Gutiérrez, F. del Río, Inorg. Chim. Acta 230 (1995) 173.
[13] A. Castellanos, J.J. García, H. Torrens, N. Bailey, C.O.R. de Barbarin, A. Gutiérrez, F. del Río, J. Chem. Soc., Dalton Trans. (1994) 2861.
[14] L.A. Oro, D. Carmona, M.P. Lamata, M.C. Apreda, C. Foces-Foces, F.H. Cano, P.M. Maitlis, J. Chem. Soc., Dalton Trans. (1984) 1823.
[15] J.J. García, H. Torrens, H. Adams, N.A. Bailey, A. Shacklady, P.M. Maitlis, J. Chem. Soc., Dalton Trans. (1993) 1529.
[16] J.J. García, H. Torrens, H. Adams, N.A. Bailey, P.M. Maitlis, J. Chem. Soc., Chem. Commun. (1991) 74.
[17] W.D. Jones, R.M. Chin, J. Am. Chem. Soc. 114 (1992) 9851.
[18] D. Carmona, M.P. Lamata, M. Esteban, F.J. Lahoz, L.A. Oro, M.C. Apreda, C. Foces-Foces, F.H. Cano, J. Chem. Soc., Dalton Trans. (1994) 159.
[19] M.P. Lamata, D. Carmona, L.A. Oro, M.C. Apreda, C. Foces-Foces, F.H. Cano, Inorg. Chim. Acta. 158 (1989) 131.
[20] A.C.T. North, D.C. Phillips, F.S. Mathews, Acta Crystallogr. A24 (1968) 351.
[21] A. Altomare, G. Cascarano, C. Giacovazzo, A. Guagliardi, J. Appl. Crystallogr. 27 (1994) 435.
[22] G.M. Sheldrick, SHELXL-93; University of Göttingen: Göttingen, Germany, 1993.
[23] International Tables for X-Ray Crystallography, Vol. 4, Kynoch Press, Birmingham, 1974.